Constraining Dark Matter Halo Mass Function down to 10^7 Msun through Strong Gravitational Lensing

Authors: Qiuhan He, David Lagattuta, Mathilde Jauzac, Tansu Daylan, Richard Massey, Jason Rhodes, Leonidas Moustakas, Alina Kiessling, Russell Smith, Stephane Werner, Satyapriya Das, et al.

Science Goal

Science Goal: Understand the nature of dark matter and its impact on the evolution (and fate?) of our universe

About 85% of all mass in the Universe is in the form of dark matter: a mysterious substance that we know almost nothing about. In our current understanding, dark matter emits no light and no energy, making it invisible to all modern detectors. Despite decades of attempts, it has never been directly observed; instead, we only see its presence indirectly, through its effects on gravity.

As the dominant mass component in our Universe, understanding the nature of dark matter is the core of our science project. Our goal, specifically, is to obtain stringent constraints on the mass of the dark matter particle by observing tiny distortions in the appearance of bright galaxies. The small-scale/low-mass objects responsible for these distortions (individual clumps of dark matter) are deeply connected to the very nature of the Universe itself. To achieve our goal, we will need extremely precise imaging, taken with an incredibly stable, high resolution camera. The stability conditions we require are only achievable from space, while HWO's unprecedented high resolution instruments are ideally matched to our imaging requirements. HWO will uniquely provide the best possible combination of instrumentation and observing conditions for our success, making it the *only* next generation telescope capable of carrying out our science.

To put our science goal in another way, **because** it interacts through gravity, dark matter is a critical component of the Universe. By dominating the mass budget, it drives the growth of all structures we can see, on all scales — from galaxies and clusters to stars, planets, and life itself. While many of many dark matter studies focus on the past (How did the universe begin? When did the first stars and galaxies form? How does structure evolve to the present day?), equally interesting are questions about the future: how will the Universe evolve, and what is its ultimate fate?)

Particularly relevant to HWO, advanced simulations suggest that without dark matter, the everyday structures we know and observe would not form. Put simply, with no dark matter, there would be no life! While life as we know it of course *does* exist, questions remain about how this life interacts with the Universe around it and what its ultimate fate will be. These answers are deeply dependent on the nature of dark matter: what dark matter *is* will affect what the Universe will *do* in the future.

Although we cannot know exactly how the universe will behave eons from now, studying dark matter will narrow the possibilities. Its properties shape the overall cosmological model, influencing both the Universe's mass fraction and its equation of state. These factors determine how the universe grows, evolves, and will continue to unfold. A better understanding of dark matter leads to better predictions of our Universe's fate.

While this goal naturally lends itself to the largest cosmological scales, we stress that small-scale structures are affected as well. There is significant literature describing the effects of dark matter on solar and planetary scale structures, though to date much of this work is limited to simulation and speculation. With the capabilities of HWO, scientists will be in a position to investigate the likelihood of small-scale events that can have a significant impact on Earth and Earth-like systems, depending on the form of the dark matter particle. Previous work has estimated that the dense dark matter clumps predicted in certain models may cross and interact with the solar system at roughly the same frequency as mass extinctions on Earth (Collar 1996). This could be due to non-gravitational interactions between dark and regular matter, which could heat up the Earth's core, leading to gigantic volcanic events (Abbas & Abbas 1998). At the same time, more recent work has also demonstrated that these particle-crossing events can alter the paths of distant comets, correctly predicting the date of the Chicxulub crater impact 66 million years ago (Kramer & Rowan 2016).

With HWO, we will explore this topic by digging into the question: What is the nature of dark matter? Understanding dark matter is considered one of the most pressing topics in modern astrophysics and cosmology in *Pathways to Discovery in Astronomy and Astrophysics for the 2020s*, and underscores one of the main priorities, i.e. question C-Q2 "What are the properties of dark matter and the dark sector?". Even more precisely, subtopic C-Q2a, "Dark sector signatures in small scale structures", highlights the importance of looking for dark matter signatures in small astrophysical objects – the **core** of this science project. Specifically, we will investigate a particularly promising dark matter candidate, and answer the question: is dark matter "warm" or "cold" and does this influence the build-up of dark matter structures (haloes) at low mass (down to the planet-mass)?

The current standard cosmology theory assumes that dark matter is “cold”: a heavy, slow-moving (compared to the speed of light) particle that only interacts through gravity. In this scenario, the structure of the universe grows in a “hierarchical” manner, with the smallest structures (dark matter haloes) forming first, then slowly merging and growing over time. Later on, gas cooled from the thermal background flows into the centers of these structures, leading to the formation of stars, planets, and the galaxies we observe today. However, despite the great success of the theory in explaining many observations, e.g. the Cosmic Microwave Background (CMB) and cosmological structures, the corresponding particles have not yet been detected in ground-based experiments, despite decades of attempts. As a result, alternative theories proposing relatively light, fast-moving particles, known as 'warm' dark matter (such as sterile neutrinos), have gained increasing attention in recent years. In the warm scenario, structure is only partially hierarchical, with smaller, lower-mass structures less common, compared to a cold Universe.

Understanding the nature of dark matter is, by extension, key to all astrophysics and astronomy fields of research, and this is exactly why we propose to investigate it with HWO and present this science project.

Science Objective

Objective: Does the hierarchical nature of dark matter structures extend to objects with masses below 10^7 M_{SUN}?

Another way to phrase our goal is to determine whether dark matter has properties other than those predicted by the standard model of cosmology, which assumes that dark matter is made of dynamically cold particles that interact only via gravity (CDM; Davis et al., 1985, Blumenthal et al., 1984). Extremely detailed models and calculations can predict the formation and gravitational evolution of structures in an expanding Universe, down to objects with Earth-like masses (10^{-6} M_{SUN}). The predictions have been successfully validated over some 4 orders of magnitude in scale, spanning the Universe’s horizon scale of 10^4 Megaparsecs (Mpc; ~3×10^{24} cm) to typical separations between galaxies, or ~1 Mpc (~3×10^{20} cm).

There are now several entire classes of dark matter candidates, increasingly well studied, that fit *current* astronomical observations on megaparsec scales and larger. Astrophysical dark matter may consist of a combination of these candidates. How do we distinguish these possible candidates? On galactic scales (and below), a discrepancy emerges between observations and theoretical models. Here, the differing properties of dark matter candidates are manifested in astrophysical processes acting at either early- or late- cosmological epochs (depending on the nature of dark matter), but which all remove small-scale, i.e. low mass, structure in the distribution of dark matter.

The standard cold dark matter (CDM) model, predicts a mass function for dark matter, i.e. the number of dark matter objects at different masses, with exponentially more clumps/structures/objects of dark matter at lower masses. A simple illustration of the dark matter mass function is shown in Figure **1**, where different mass functions predicted by various warm dark matter candidates are compared to the reference CDM case (in black). Alternatives to CDM, such as warm, wavelike, decaying, or self-interacting dark matter, all smooth out and remove clumps of dark matter with mass below a characteristic cut-off scale. The cut-off value, $m_{cut\text{-}off}$, inversely depends on the specific particle mass, m_{DM}, as:

$$m_{\mathrm{cut-off}} = 10^{10} \left(\frac{m_{\mathrm{DM}}}{1\mathrm{keV}} \right)^{-3.33} \mathrm{M}_{\odot}\mathrm{h}^{-1}$$

where h is the dimensionless Hubble constant. As indicated, the larger the particle mass, the smaller the cut-off for the halo mass function. Nowadays, most interesting alternative dark matter models predict a cut-off mass below ~ 10^8 M_{sun}. Our objective, then, is to identify and classify dark matter clumps below this characteristic cutoff. In doing so, we will answer the question regarding the hierarchical behavior of dark matter, allowing us to better constrain its physical properties.

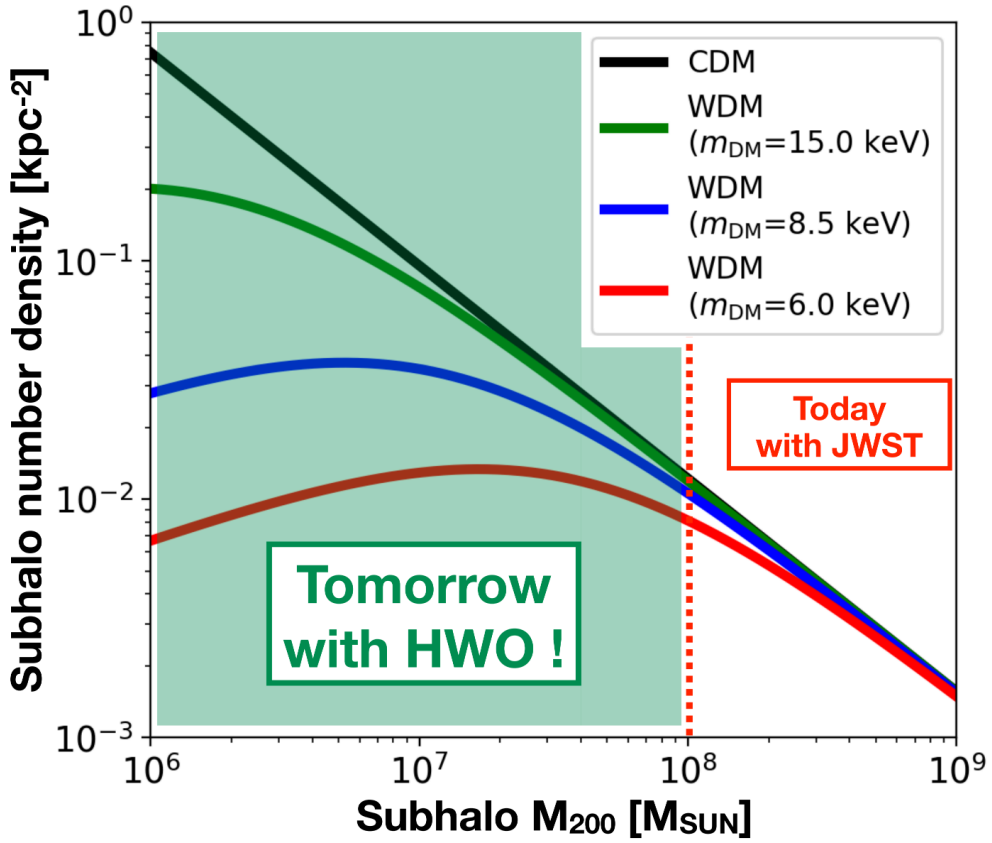

Figure 1: *Predicted subhalo mass function of dark matter in several dark matter models. The mass function simply shows the expected number of objects (in a given volume) that have a given mass. While all cosmologies predict similar numbers of objects of higher masses (> 10^8 M_{SUN}), this behavior changes at lower masses. In the*

standard LCDM cosmology (black curve), the number density continuously increases as the object mass decreases (down to around the Earth mass). Conversely in alternative models, the number density is suppressed, though the level of suppression, and the mass range where this occurs, is tied to the dark matter particle mass.

At the time of HWO, the most exciting measurement will be

(1) Detecting hundreds of thousands of dark matter haloes down to ~ 10^7 M_{SUN} and resolving their internal structure, e.g. compactness of those haloes.

- The best achievements so far are 3 detections with masses over 10^9 M_{SUN} (Vegetti et al. 2009, 2012; Hezaveh et al. 2016).
- Minor et al. (2021) showed that one of the 3 detected subhalos has an extremely compact structure which can be hardly explained by the standard/CDM model, but might be due to the gravothermal collapse of strongly self-interacting dark matter. ***Measurements of the internal structures of small halos can reveal additional constraints on the nature of dark matter.***

(2) Measuring the dark matter subhalo/line-of-sight mass function down to the 10^7 M_{SUN} regime at different redshifts

- Cyr-Racine et al. (2015) developed the Effective THeory Of Structure Formation (ETHOS) which predicts turn-offs of the halo mass function of popular dark matter models.
- Dhanasingham et al. (2023) showed that distinguishing the line-of-sight small dark matter haloes from the lens subhaloes was possible.
- ***A significant fraction of the parameter space of various dark matter models will be tightly constrained by measuring the halo mass function down to this mass range.***
- ***A census of small dark matter haloes at different redshifts will provide a much clearer picture of the formation and evolution theory of the structure of the Universe.***

Step 3: Physical Parameters

<u>Parameters</u>: Number and mass of small (sub-galactic) dark matter objects down to ~ 10^7 M_{SUN}

As shown in Figure **1**, the dark matter mass function has a characteristic cut-off scale at which the number of dark matter objects will differ between different dark matter candidates. Alternative popular candidates, like sterile neutrinos of several keVs, predict no existence of haloes below ~ 10^6-10^{10} M_{SUN} (depending on the

specific mass values). So our observation aims to search for dark matter objects of the lowest possible masses, with an HWO limit estimated from our simulations of 10^7 M_{SUN}. *We will measure the abundance and properties of these dark matter structures, starting with their mass.* ***The most promising tool*** *that can be used to map dark matter indirectly is called* ***gravitational lensing***.

According to Einstein's theory of General Relativity, massive objects like galaxies or galaxy clusters can bend and distort the light coming from more distant galaxies behind them—a phenomenon known as gravitational lensing. This effect creates stretched or duplicated images of the background galaxy and lets scientists "see" the total mass of the foreground object, including the invisible dark matter. In strong lensing, these distortions become dramatic, forming arc-like shapes. Small clumps of dark matter, even if they contain no stars, can create additional changes in these arcs, such as shifting their positions or brightness (see **Figure 2** for a demonstration). By carefully studying many of these lensing effects, scientists can detect and measure the amount and size of small dark matter structures throughout the universe.

Our ultimate goal is to detect low-mass ($10^6 < M_{sun} < 10^8$) dark matter structures and characterize their mass function. This will allow us to robustly discriminate between predictions of CDM and its neutrino alternatives (see Figure **1**, and discussion in Viel et al. 2013 and Lovell et al. 2014). To achieve this goal, we will need to detect and measure the masses of individual dark matter (sub)haloes in sufficient numbers (thousands) to generate an accurate mass function of the full population.

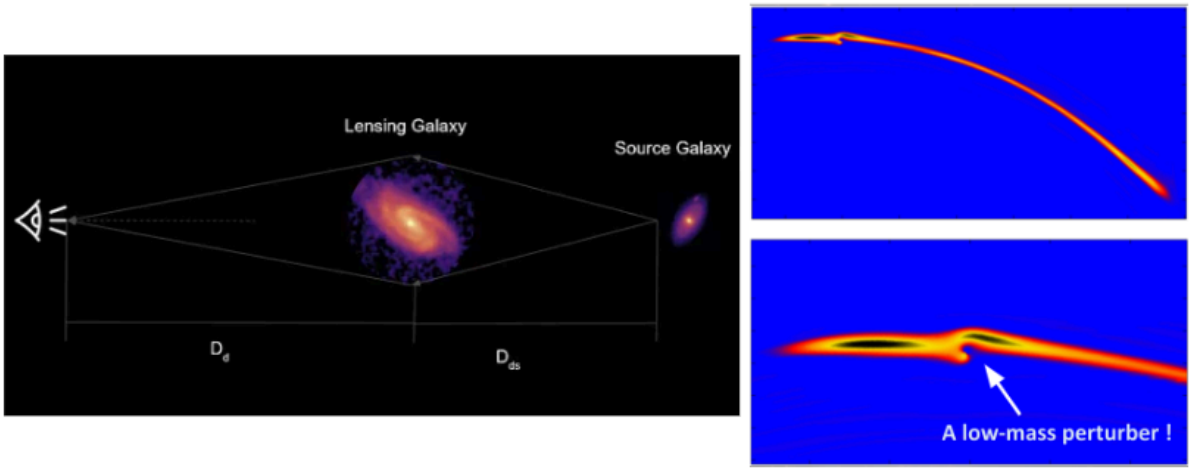

Figure 2: *Examples of gravitational lensing and gravitational imaging.* ***Left****: a geometric diagram of gravitational lensing, demonstrating how light from a distant source galaxy is deflected by a massive intermediate (lens) galaxy on its way to an observer. Picture from* ***Towards Data Science***[1]*.* ***Right****: a simulation of the gravitational imaging effect. If an additional mass lies close to the image of the*

[1] https://towardsdatascience.com/reconstruct-source-galaxy-images-from-strong-gravitational-lens-images-using-u-net-1d8221100601

source galaxy (though this mass can be anywhere along the line of sight) it will cause a noticeable additional distortion in the arc. The strength of this distortion is due to a combination of distance and mass and can be used to estimate the mass of the perturber. Picture modified from McKean et al. 2015.

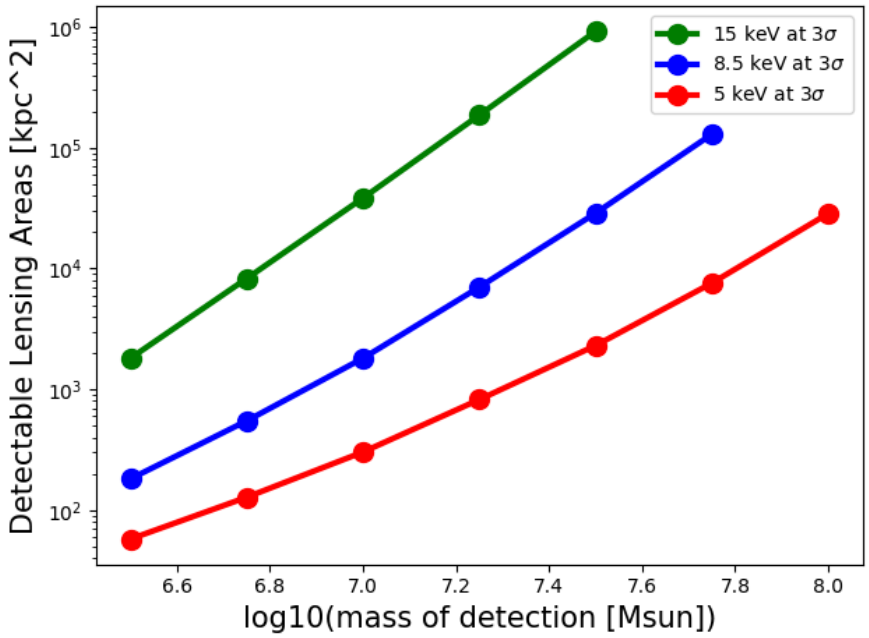

Figure 3: *The detectable lensing areas required as a function of the lowest detectable halo mass to achieve a 3-sigma constraint on the dark matter models with different particle masses. Red, Blue, and Green curves show the requirement for constraining the dark matter model with a particle mass of 5.0, 8.5, and 15.0 keV, respectively.*

The final constraint on dark matter particle mass we could obtain is directly linked to the detectable halo masses and their corresponding areas. Specifically, assuming a CDM universe, the expected number of detectable low-mass halos with masses larger than m_{low} can be expressed as:

$$N_{\mathrm{exp,CDM}} = \int_{m_{\mathrm{low}}} F_{\mathrm{CDM}}(m)dm \cdot A$$

where F_{CDM} is the CDM mass function (in terms of the area), and A is the detectable area associated with a halo mass greater than m_{low} (the upper value is set to be 10^{10} M_{SUN} here). Similarly, we can compute the number of detectable low-mass haloes of a given WDM model as

$$N_{\mathrm{model,WDM}} = \int_{m_{\mathrm{low}}} F_{\mathrm{WDM}}(m)dm \cdot A$$

The χ^2 difference between the expected CDM model and the tested WDM model can then be computed as:

$$\chi^2 \equiv \frac{(N_{\mathrm{exp,CDM}} - N_{\mathrm{model,WDM}})^2}{N_{\mathrm{exp,CDM}}}$$

To rule out a given WDM model at a certain significance level, the relationship between the detectable halo mass, $m_{low,}$ and its associated area A can be derived as:

$$A = f(m_{\rm low})|_{\chi^2=C},$$

where C depends on the desired significance level. For convenience and following common astronomical practice, we set the significance threshold to be 3-sigma for our estimates. Throughout this analysis, we assume the Universe follows the CDM model. As a demonstration, Figure **3** calibrates the required detectable lensing area, as a function of the detectable halo mass needed to achieve a 3-sigma constraint on the particle mass of dark matter, if dark matter is warm. The detectable lensing area at a given subhalo mass means the area of the regions where we have the sensitivity to detect a subhalo of the given mass.

In practice, we will point HWO at individual strong lensing systems and search for dark matter haloes around lensed images. Depending on the specific lensing configurations, within a single lensing system, the lowest detectable dark matter halo mass varies across different regions of the lensed images. To estimate the number and mass of low-mass haloes that can be detected in a typical strong lensing system, we derive sensitivity maps for different imaging resolutions. We do this by fitting mock images with a low-mass halo at various locations around the lensing arc (for details, see Amorisco et al. 2021, and He et al. 2022).

In Figure **4**, we show examples of the sensitivity maps for a mock imaging resolution of 0.007 arcsecs. The color of each grid indicates the detectability of a low-mass dark matter halo of a given mass (left: 10^7 M_{SUN}; right: $10^{7.25}$ M_{SUN}) at the center of that grid. The detectability value in each grid is determined in three steps:

(1) Creating a mock image with a low-mass halo located at the center of the grid.

(2) Fitting the mock image with two different models: one using only a smooth macro model (without a low-mass halo) and the other one including a low-mass halo.

(3) Computing the maximum log-likelihood difference between the two fits in step 2, which serves as an indicator of the detectability of the low-mass halo at that grid point.

A log-likelihood difference of 5 corresponds to 3-sigma significance. Throughout the analysis, we consider a halo detectable if the log-likelihood difference exceeds 5.

Currently, computing the sensitivity maps is a time-consuming task due to the large variability in the parameter space, including different observational setups and various combinations of low-mass halo masses and locations. To make the task manageable, we compute sensitivity maps for four imaging resolutions of interest — 0.005”, 0.007”, 0.01”, and 0.03”. For each resolution, we compute the maps for a typical lensing configuration, assuming a lens at a redshift of 0.2, and a source at a redshift of 0.6. The source is simulated as a bright Lyman-alpha emitter composed of several sub-kpc clumps with a total apparent UV magnitude of ~ 22. We set the

depth of the mock images to have a total signal-to-noise ratio (S/N) of ~ 2500. According to the LUVOIR Exposure Time Calculator (ETC), for an 8-meter telescope, reaching this depth requires approximately 2 hours of observing time.

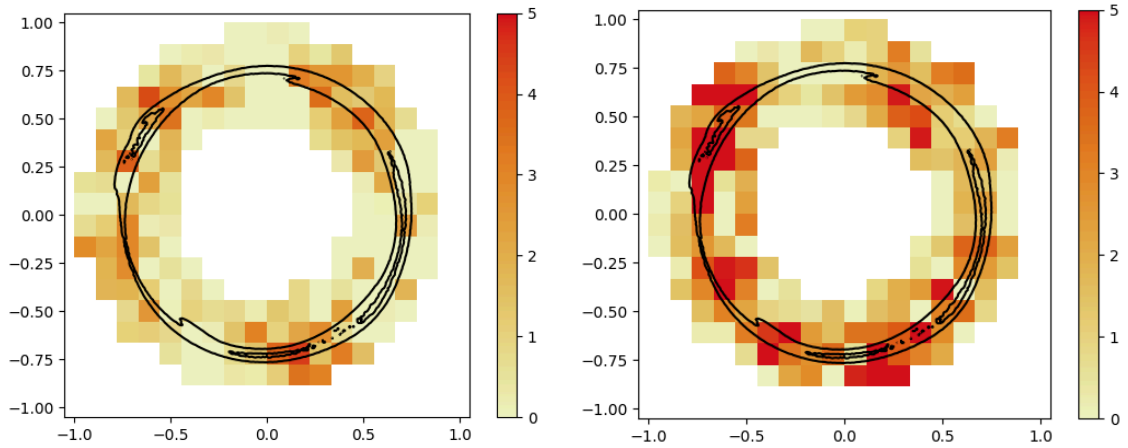

Figure 4: *Example sensitivity maps for an imaging resolution of 0.007". The color in each grid point represents the detectability of a low-mass perturber of a given mass (**Left panel**: 10^7 M_{SUN}; **Right panel**: $10^{7.25}$ M_{SUN}) at the center of that grid. Detectability is calculated as the maximum log-likelihood difference between fitting mock images with a smooth model (without a low-mass halo) and a model that includes a low-mass halo. A value greater than 5 corresponds to an over 3-sigma significance, indicating that a halo located in the grid is detectable. In the left panel, no grid point has a value greater than 5, indicating that this setup cannot detect a 10^7 M_{SUN} halo. However, in the right panel, 15 grid points show values greater than 5, demonstrating that in certain regions around the lensing arc, a slightly larger halo with a mass of $10^{7.25}$ M_{SUN} can be detected. The solid black contours outline the lensing arcs. The lens redshift is 0.2, and the source redshift is 0.6. The x- and y-axis units are in arcseconds.*

We consider five specific halo masses: 10^7, $10^{7.25}$, $10^{7.5}$, $10^{7.75}$, and 10^8 Msun. When creating the sensitivity maps, we assume that all low-mass haloes are located in the lens plane. However, low-mass haloes along the line of sight could also contribute to the detection. Based on previous studies (He et al. 2022), we approximate the contribution from line-of-sight haloes to be roughly equivalent to that of haloes located on the lens plane.

By integrating the sensitivity maps shown in Figure **4** with the halo mass function from Figure **3**, we can compute the expected number of detectable haloes for different dark matter models at various imaging resolutions. For example, in Figure **5**, we show the expected number of dark matter haloes (across different mass ranges) detectable by observing 1,000 lensing systems for two models: CDM (left) and WDM with a particle mass of 8.5 keV (right).

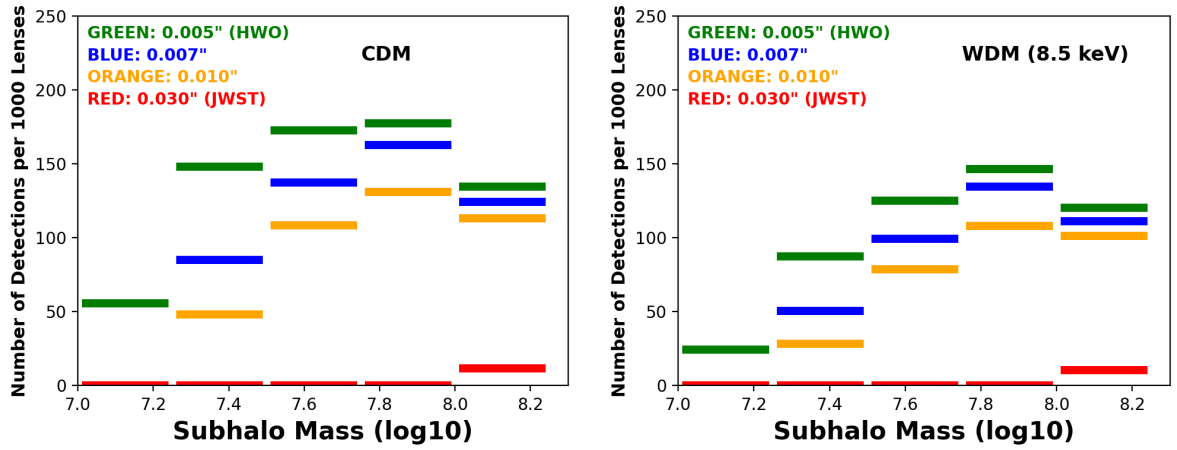

Figure 5: *Expected detectable numbers of dark matter haloes per 1,000 lensing systems under different resolutions (green, blue, orange, and red correspond to an imaging resolution of 0.005", 0.007", 0.010", and 0.030" respectively) and dark matter models.* ***Left:*** *the CDM case.* ***Right:*** *the WDM (m_{DM} = 8.5 keV) case.*

Using these histograms, we can modify our previous χ^2 equation to calculate the significance of ruling out WDM models with a specific particle mass:

$$\chi^2 \equiv \sum_i \frac{\left(N^{m_i}_{\text{exp,CDM}} - N^{m_i}_{\text{model,WDM}}\right)^2}{N^{m_i}_{\text{exp,CDM}}},$$

where m_i represents different halo masses (e.g. the mass bins in Figure **5**). Using these equations, we can determine the scientific return based on different numbers of observations and imaging resolutions, which are summarized in Table **1**.

Table 1: *Physical parameters*

Physical Parameter	**State of the Art**	**Incremental Progress (Enhancing)**	**Substantial Progress (Enabling)**	**Major Progress (Breakthrough)**
Number of Objects (Extended lensing arc)	100	500	1000	2000
Resolution	0.03"	0.01"	0.007"	0.007"
Subhalo mass range (Msun)	> 10^8	> 5x10^7	> 2x10^7	> 2x10^7
Confidence of detection	3 sigma at 3.2 keV	3 sigma at 9.2 keV	3 sigma at 11.0 keV	3 sigma at 12.3 keV

Step 4: Description of Observations

Observations: Imaging & Spectroscopy of extended gravitational lensing arcs

As described above, our primary mode of detection is through strong gravitational lensing imaging (Vegetti et al. 2009). To maximize the efficiency of gravitational imaging, we require simultaneous astronomical imaging and spectroscopic information. While this is possible even today, the level of precision we can currently achieve is not sufficient to discriminate between models in a meaningful way. The measurement precision is mainly driven by the data quality of the imaging, especially the imaging resolution and stability of the PSF, and the number of targets.

The main competitors of HWO will be ground-based, next-generation facilities (NGFs) such as the ELT, GMT, and TMT. These observatories are expected to achieve resolutions similar to those of HWO, albeit restricted to longer-wavelength regimes. However, as a space-based telescope, HWO provides an extremely stable PSF across a wide range of wavelengths. In contrast, although NGFs can approach diffraction-limited resolution with adaptive optics, atmospheric turbulence still introduces significant variations in the point spread function during long exposures. This presents challenges when processing observed data, especially for tasks that require extracting tiny perturbations in lensed images caused by low-mass dark matter haloes (Galan et al. 2024). Furthermore, the laser-based AO corrective systems employed by NGFs will necessarily create gaps in wavelength coverage, reducing the available redshift space for detecting lenses. Along similar lines, a space-based instrument such as HWO will not be affected by correlated atmospheric noise, making it easier to detect low-level signals. **This will, by comparison, be a challenge for NGFs** (Föhring et al. 2019, Beesley et al. 2024).

Currently, the best *JWST* observation with a resolution of 0.03” can detect dark matter objects down to ~ 10^8 M_{SUN}. A very high-resolution interferometry telescope like VLBI – with mliliarcsec resolution – can push the detection down to <~ 10^7 M_{SUN}; This is already in a mass regime that can discriminate between the standard cold dark matter and its interesting alternatives. However, using VLBI alone, we ***cannot*** measure a robust census of small-scale masses. This is because lensing arcs in millimeter bands are exceptionally rare: radio-loud background sources are usually energetic jets emitted from the center of galaxies; as of today no more than 30 of these sources have been discovered across the sky. At the same time, the high-sensitivity region of these arcs is extremely narrow, limiting their utility. By contrast, a high-resolution combined with additional observational constraints makes HWO the ideal and unique telescope to achieve the scientific objective. With HWO, we expect to push the lower boundary down to the 10^7 M_{SUN} regime with a sufficient number of lensing arcs observable in the UV bands.

We, below, describe the details of the set-ups we require in terms of both imaging or integral field spectroscopy.

Broad- and narrow-band Imaging

- ***Resolution***
  The resolution is the fundamental parameter to determine the precision of our measurement. Its relation to the lowest detectable subhalo mass is calibrated as shown in Figure **6** through imaging simulations. As shown, the lowest detectable mass for our mock simulation is 10^7, $10^{7.25}$, $10^{7.5}$, $10^{7.75}$, and 10^8 M_{SUN} for an imaging resolution of 0.005", 0.007", 0.010", and 0.030" respectively.

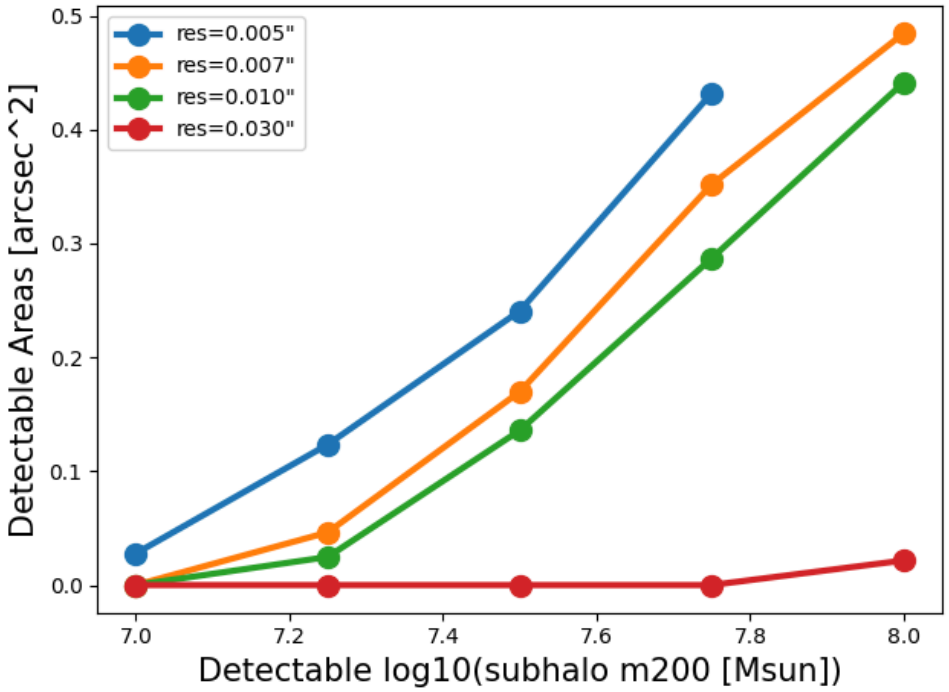

Figure 6: *Lowest detectable dark matter halo masses and their associated detectable areas in the mock lensing system demonstrated in* ***Figure 4****. Different colors represent different assumptions for imaging resolutions.*

- ***Field of View (FOV)***
  For strong gravitational lensing, we are considering three types of FOVs, which correspond to three different lensing scales depending on the foreground lens objects, galaxy, group, and galaxy cluster scales. Because our scientific objective is directly linked to the lensing areas one could observe. A larger FOV that could observe multiple lensing arcs/areas at once could be more efficient for our observational task. In the Table below, we summarize the FOVs required to observe the three types of lensing systems and the corresponding lensing areas in the systems.

Lensing Types	Galaxy Scale	Group Scale	Cluster Scale
Typical Lensing Areas	1 kpc^2	5 kpc^2	100 kpc^2
FOV required	20x20 $arcsec^2$	60x60 $arcsec^2$	200x200 $arcsec^2$

The minimum requirement is to cover a typical galaxy-galaxy lens system < 20x20 $arcsec^2$. However, we see a possibility that we can achieve the equivalent goal (searching the same size of areas covered by lensing arcs) more efficiently (meaning more detectable areas with the same exposures) by targeting lensing arcs within a cluster lensing system, which usually spans several arcminutes across the sky.

- ***Wavebands***
  Wavebands limit the maximum redshifts of sources we can observe and thus the total number of lenses feasible. For example, if we want to target Ly-alpha emissions, which are bright and clumpy (good for subhalo sensitivity), then we can relate the waveband range to the maximum redshifts we can observe, which is further related to the number of systems we can observe. In the following table, we compute, under different maximum wavelengths, the maximum source redshifts we can target for different types of lenses.
- ***Precise knowledge of the Point Spread Function (PSF)***
  Knowledge of the PSF (either because it is stable or can be modeled) is crucial for accurately modeling low-mass perturbations to lensed images. Galan et al. (2024) have shown that an inaccurate PSF model could lead to biases in the properties of the main lens galaxy, especially when the sources are clumpy and cuspy. The requirement for a stable PSF is the reason why the space-based HWO is necessary for our scientific goal compared to ground-based telescopes like ELT. A full evaluation of the required HWO PSF stability required for this science case is a task for future work.
- ***Methodology and data analysis techniques***
  To simulate the performance of HWO in this document, we have assumed that low-mass dark matter perturbers must be detected individually. This is a challenging measurement; Gilman et al. (2020) have shown that more advanced lensing data analysis techniques, such as simulation-based inference, should achieve a factor 5-10 greater sensitivity (in terms of the low-mass halo masses) by instead searching for the ensemble population of perturbers below a given mass. Such methods will have been perfected before the launch of HWO, so we expect the lensing observations would give even tighter constraints than the predictions given in this document.

Integral Field Unit (IFU) Spectroscopy

In addition to waveband imaging, IFU spectroscopy from HWO would significantly increase the return on our science case. IFU data will complement broadband imaging in two key ways: 1.) spectroscopic data will provide critical redshift data, and 2.) 2-dimensional spectroscopic (IFU) imaging will allow us to isolate the emission-line flux of the source, reducing contamination from the lens galaxy continuum flux, as well as the time needed to reach a desired SNR.

- ***FOV***
  Ideally the IFU FOV will match the entire strong lensing region in the case of galaxy-scale lenses and (at the very least) the extent of a lensed arc in groups and clusters. For galaxy-scale lenses, a FoV of ~10 arcsec^2 should be more than enough (this will cover the lens and spectroscopically confirm any nearby structure/galaxies). A ~1 arcmin^2 FOV would cover an entire galaxy group, as well as the complete strong-lensing region of galaxy clusters. This would allow for "blind" detection of lensed arcs without a strong continuum, increasing our available lens sample by up to 50-100% (Mahler et al. 2018).
- ***Resolution***
  Unlike spatial resolution, spectral resolution is not as large a driver for our science case, though we note there are advantages to a high R dispersion. In particular, higher resolving power will allow us to precisely separate individual kinematic components of the gas. This means we can highlight individual nebular knots in the gas cloud, providing hundreds of unique sight lines to probe for substructures.

- ***Wavelength Coverage***
  Once again, the IFU wavelength coverage will dictate which targets we can detect. In the following table, we compute the maximum source redshifts we can target for different emission lines, given a short-wavelength starting point of 2000 Angstroms – the nominal blue-cutoff for the HWO UV spectrograph.

Table 2: *Maximum observable redshifts (based on wavelength upper-limit). A wavelength coverage of 2000-6100 A would completely eliminate redshift "deserts" in HWO (redshifts where no strong emission features fall into the wavelength range). Colors indicate the number of expected lens detections (Red: < 500; Yellow: 500 - 2000; Green: > 2000).*

	2000 A	3000 A	4000 A	5000 A	6000 A	7000 A
Ly-a	0.65	1.47	2.29	3.11	3.94	4.76
[OII]	N/A	N/A	0.07	0.34	0.61	0.88

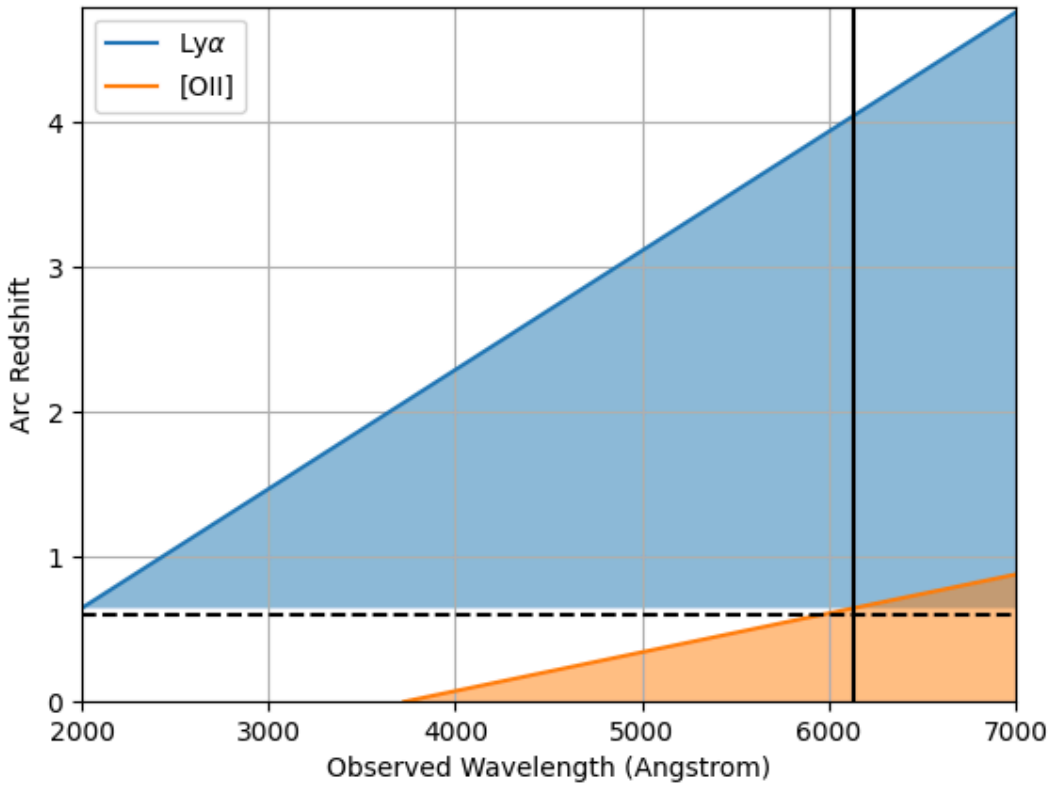

Figure 7: *Redshift coverage with an HWO (IFU) spectrograph. This is a diagrammatic representation of the above table. The dashed horizontal line (z = 0.6) is roughly double the redshift of the average gravitational lens (z_{lens} ~ 0.3). Objects beyond this distance have a very high probability of being lensed efficiently. Colored lines show the highest possible redshift that can be observed (for a given spectral line) as a function of wavelength. The shaded regions show all achievable redshifts, assuming a blue-side cutoff of 2000 Angstroms. Areas in white are redshifts that are either physically inaccessible (above the blue line) or difficult to detect (between the colored regions), due to a lack of bright lines (those with high SNR and high Equivalent Width) in the wavelength region. These gaps are known as "redshift deserts" (e.g., Renzini & Daddi 2009), and will limit our ability to identify and confirm lenses. The solid vertical line marks the elimination of this desert, which would considerably benefit this science case.*

As HWO is a UV-capable telescope, we only consider two types of lenses with emissions in short wavebands, the Ly-alpha and [OII] emitters, for now as shown in Figure **7**. For those two types of lenses, in Figure **8**, we further quantify the number of expected lens systems as a function of the maximum wavebands.

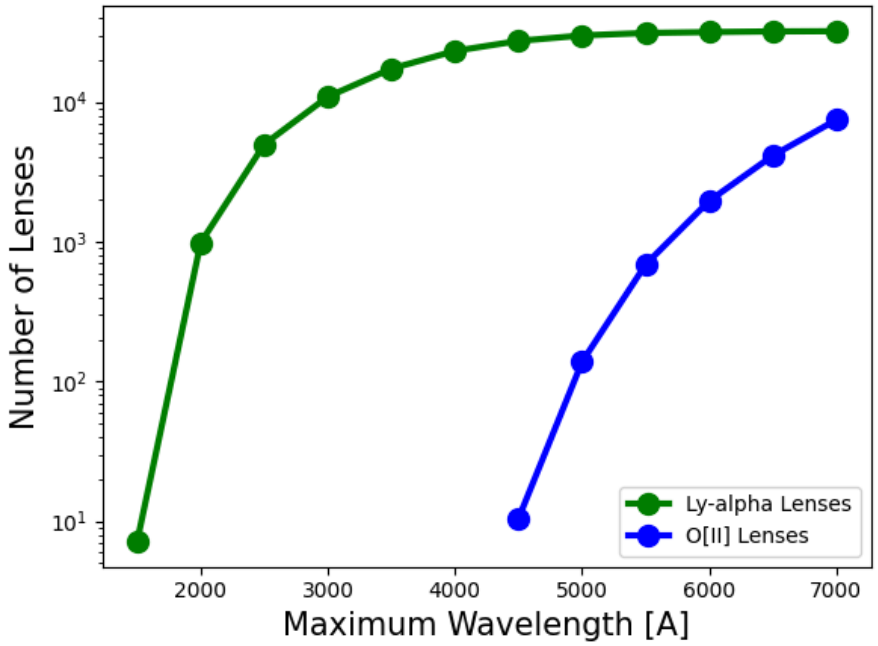

Figure 8: *Number of lenses as a function of the maximum wavelength. Green and blue curves show the relations for Ly-alpha and [OII] lenses respectively.*

For a given telescope aperture, the imaging resolution is inversely proportional to the observed wavelength (and thus the number of detectable lenses). So, to maximize our scientific achievement, we need to achieve a balance between the resolution and the wavelength. Also, the number of detectable lenses is limited by the total project hours. As mentioned, we estimate ~ 2 hours exposure for one lensing system, which means for a reasonable project of 1000 hours, we are able to observe 500 lensing systems if not limited by wavelengths. Taking into account the telescope aperture, resolution, and total project hours, we derive the expected 3-sigma constraints on the particle mass in Figure **9** (assuming we are in a CDM universe). For clarity, we also summarize those constraints in Table **3**.

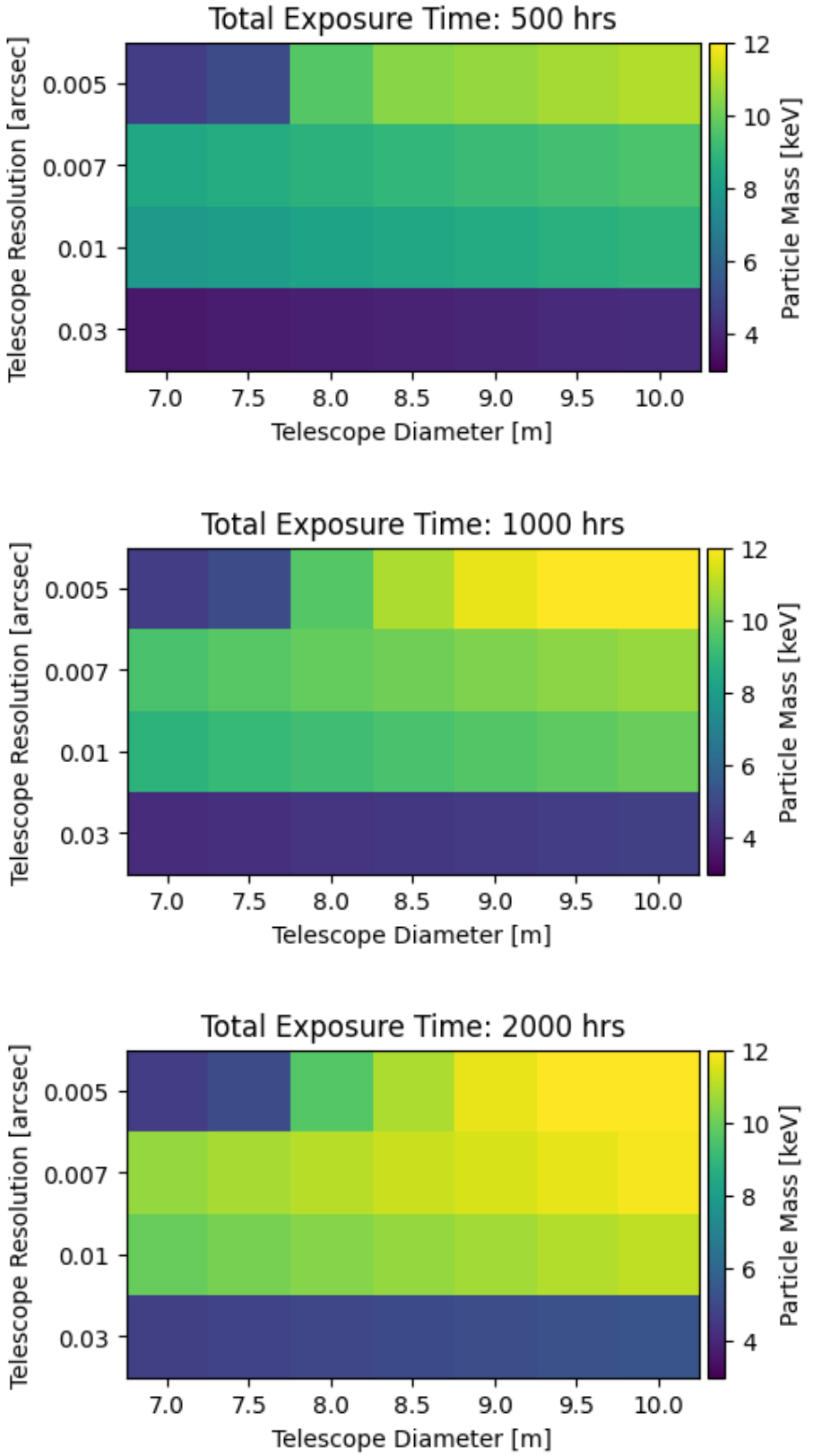

Figure 9: *Expected 3-sigma constraints as a function of mission parameters and the total project hours. The colors show the expected 3-sigma constraints on the dark matter particle mass.*

Table 3: *Constraining power for different telescope set-ups as a function of exposure times. Green cells mark where we can reach a mass limit >10 keV for each aperture.*

Maximum Total Exposure: 500 hrs							
	7.0 m	7.5 m	8.0 m	8.5 m	9.0 m	9.5 m	10.0 m
0.005”	4.6	5.1	9.6	10.4	10.6	10.8	11.0
0.007”	8.3	8.6	8.8	9.0	9.1	9.3	9.5
0.01”	7.8	8.0	8.2	8.4	8.5	8.7	8.9
0.03”	3.6	3.7	3.8	3.9	4.0	4.1	4.2

Maximum Total Exposure: 1000 hrs							
	7.0 m	7.5 m	8.0 m	8.5 m	9.0 m	9.5 m	10.0 m
0.005”	4.6	5.1	9.6	10.9	11.7	12.1	12.3
0.007”	9.4	9.7	9.9	10.1	10.3	10.4	10.6
0.01”	8.8	9.0	9.2	9.4	9.6	9.8	9.9
0.03”	4.1	4.2	4.3	4.4	4.5	4.6	4.7

Maximum Total Exposure: 2000 hrs							
	7.0 m	7.5 m	8.0 m	8.5 m	9.0 m	9.5 m	10.0 m
0.005”	4.6	5.1	9.6	10.9	11.7	12.3	12.7
0.007”	10.6	10.8	11.0	11.3	11.5	11.7	11.9
0.01”	9.9	10.1	10.4	10.6	10.8	10.9	11.1
0.03”	4.7	4.8	4.9	5.0	5.1	5.2	5.3

Interestingly, recent X-ray observations of a 3.55 keV emission line from Galactic Center have brought attention to a popular physically-motivated warm dark matter candidate known as sterile neutrinos, which can generate X-ray emissions through radiative decay. Depending on the specifics of the decay mechanism, the mass of sterile neutrinos can range from several keV to ~ 20 keV, with the upper limit constrained by the risk of overproducing X-ray emissions (Adhikari et al. 2016). For instance, if the 3.55 keV line arises from a two-body decay process, the sterile neutrino particle mass would be around 7.1 keV, corresponding to a cut-off mass of ~ 2 x 10^7 M_{SUN} (de Vega et al. 2014). This mass range aligns perfectly with the predicted constraining power shown in our tables, making the HWO an ideal facility

for detecting or ruling out sterile neutrino candidates. Moreover, if we can push our constraints beyond 10 keV (highlighted in green in the tables) and combine them with X-ray constraints, we stand at the brink of a transformative discovery. Such an achievement would leave little room for the sterile neutrino hypothesis to escape scrutiny—or, perhaps more thrillingly, offer us an unprecedented opportunity to confirm that dark matter is indeed composed of sterile neutrinos.

Throughout this proposal, we have limited ourselves to the discussion of detecting individual dark matter haloes. However, this is not the only application of this science case. Studies have shown that additional constraints can be obtained through statistical methods, particularly by analyzing the power spectrum of lensed image residuals (He et al. 2022). In principle, this technique can *provide even stronger constraints* on the dark matter particle mass relative to detecting individual dark matter haloes. We note, too, that correlated atmospheric noise present in NGF data would be an even greater challenge in this case, as it is extremely hard to cleanly isolate and model low-mass dark halo residuals in the presence of atmospheric noise. While the exact details of these techniques are still being developed, by the time of HWO they will be fully vetted and a robust, complementary tool in our arsenal. We thus stress that the numerical estimates presented here can **only improve**. Having a telescope with a UV-optimized imager and broad IFU spectrograph will therefore cement the legacy of HWO as a truly transformative facility for dark-sector astrophysics, one of the main priorities of the *Pathways to Discovery in Astronomy and Astrophysics for the 2020s*.

Table 4: *Imaging Observation*

Observation Requirement	**State of the Art**	**Incremental Progress (Enhancing)**	**Substantial Progress (Enabling)**	**Major Progress (Breakthrough)**
Type (imaging, spectroscopy, etc.)	Imaging ***JWST***	Imaging ***JWST drizzled & deep***	Imaging ***ELT/AO & WST/AO***	Imaging ***HWO***
Wavelength Range	Visible/IR (0.6 - 5 μm)	Visible/IR (0.6 - 5 μm)	UV/Visible/IR (0.3 - 2.5 μm)	UV/VIsible (~ 200 - 500 nm)
Amount of sky covered	4x4 arcmin^2	4x4 arcmin^2	53x53 arcsec^2 & 3x3 arcmin^2	4x4 arcmin^2 (e.g. tiled observarions)
Magnitude of target in chosen bandpass	29	30	35	35
Angular resolution	0.05”	0.03”	0.01”	0.005” - 0.007”

Table 5: *Spectroscopic Observation*

Observation Requirement	**State of the Art**	**Incremental Progress (Enhancing)**	**Substantial Progress (Enabling)**	**Major Progress (Breakthrough)**
Type (imaging, spectroscopy, etc.)	Spectroscopy IFU ***VLT/IFU***	Spectroscopy IFU ***VLT/IFU deep + AO***	Spectroscopy IFU ***ELT/IFU & WST/IFU***	Spectroscopy IFU ***HWO/IFU***
Wavelength Range	Visible/IR	Visible/IR	UV/Visible/IR	UV/Visible
Amount of sky covered	1x1 arcmin^2	1x1 arcmin^2	3x4 arcsec^2 & 3x3 arcmin^2	60x60 arcsec^2
Magnitude of target in chosen bandpass	26	28	30	30
Angular resolution	0.2”	0.15”	0.04”	0.02”
Spectral resolution	1700-3700	1700-3700	3200-17000 & 3500	10000